LANGMUIR

pubs.acs.org/Langmuir Article

Collagen Networks under Indentation and Compression Behave Like Cellular Solids

Published as part of Langmuir virtual special issue "2023 Pioneers in Applied and Fundamental Interfacial Chemistry: Nicholas D. Spencer".

Christopher S. O'Bryan, Yongliang Ni, Curtis R. Taylor, Thomas E. Angelini, and Kyle D. Schulze*

Cite This: *Langmuir* 2024, 40, 4228–4235 Read Online

ABSTRACT: Simple synthetic and natural hydrogels can be formulated to have elastic moduli that match biological tissues, leading to their widespread application as model systems for tissue engineering, medical device development, and drug delivery vehicles. However, two different hydrogels having the same elastic modulus but differing in microstructure or nanostructure can exhibit drastically different mechanical responses, including their poroelasticity, lubricity, and load bearing capabilities. Here, we investigate the mechanical response of collagen-1 networks to local and bulk compressive loads. We compare these results to the behavior of polyacrylamide, a fundamentally different class of hydrogel network consisting of flexible polymer chains. We find that the high bending rigidity of collagen fibers, which suppresses entropic bending fluctuations and osmotic pressure, facilitates the bulk compression of collagen networks under infinitesimal applied stress. These results are fundamentally different from the behavior of flexible polymer networks in which the entropic thermal fluctuations of the polymer chains result in an osmotic pressure that must first be overcome before bulk compression can occur. Furthermore, we observe minimal transverse strain during the axial loading of collagen networks, a behavior reminiscent of open-celled cellular solids. Inspired by these results, we applied mechanical models of cellular solids to predict the elastic moduli of the collagen networks and found agreement with the moduli values measured through contact indentation. Collectively, these results suggest that unlike flexible polymer networks that are often considered incompressible, collagen hydrogels behave like rigid porous solids that volumetrically compress and expel water rather than spreading laterally under applied normal loads.

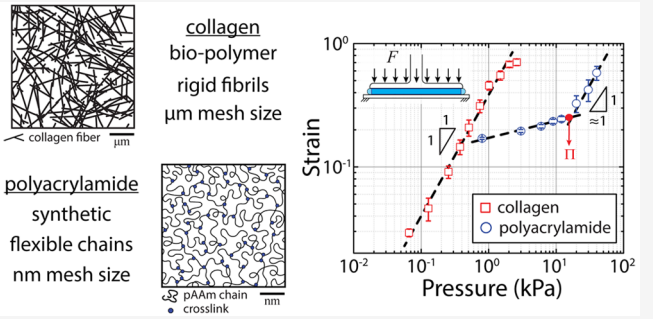

INTRODUCTION

Biomedical implants, engineered tissue constructs, and experimental surrogates for tissues are often made from synthetic or biopolymer hydrogels.[1−8] Cross-linked polyacrylamide (pAAm) is one of the most commonly employed synthetic hydrogels and has been widely applied in molecular biology, cell mechanics studies, *in vitro* tribological models, and biomedical implants,[9−13] while branched collagen networks are among the most commonly employed biopolymer hydrogels in tissue engineering, biomaterials science, and cell biology.[14−19] Both pAAm and collagen hydrogels are often chosen as experimental tissue surrogates due to their ability to tune their elastic moduli and hydraulic permeabilities to mimic those of real tissues.[12,13,20−24] However, these two hydrogels represent two distinct classes of polymer networks which differ fundamentally in their microstructural and nanostructural makeup and their response to applied forces.[25−30] Synthetic hydrogels, such as pAAm, are frequently made from flexible polymers prepared in the semidilute polymer regime, while many biopolymer hydrogels are made from semiflexible or rigid polymers (Figure 1).[31−35] Thus, the material and transport properties that separate these categories of polymer network must be investigated and compared to interpret their mechanical performance in current applications and to guide the development of new applications.

Recently, we showed that pAAm hydrogels are nearly incompressible when the applied pressure is less than the polymer osmotic pressure.[36] The underlying mechanism of this incompressibility lies in the thermal fluctuations of the flexible polymer chains as they begin to overlap in the semidilute polymer regime as famously described by DeGennes. Within

Received: November 2, 2023
Revised: January 25, 2024
Accepted: January 25, 2024
Published: February 15, 2024

https://doi.org/10.1021/acs.langmuir.3c03357
Langmuir 2024, 40, 4228−4235

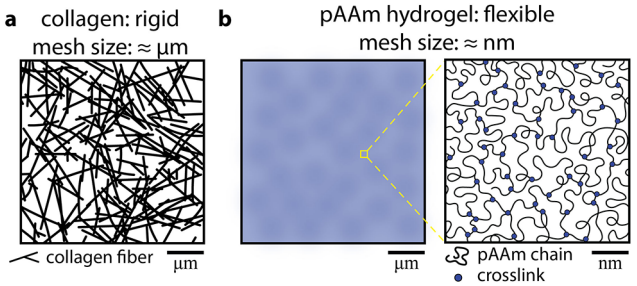

Figure 1. Schematics of two types of hydrogel networks commonly used as tissue surrogates. (a) Glutaraldehyde cross-linked collagen networks are rigid biopolymer hydrogels consisting of fibers with mesh sizes on the order of micrometers. (b) pAAM is a synthetic hydrogel consisting of flexible polymer chains with mesh sizes on the order of nanometers.

this semidilute regime, the osmotic pressure scales like $\Pi = k_B T/\xi^3$, where k_B is Boltzmann's constant, T is the temperature, and ξ is the mesh size of the polymer network. ξ is generally on the order of nanometers for pAAm hydrogels. In contrast, collagen networks typically consist of rigid fibers that form branched networks with micrometer-scale mesh sizes. We hypothesize that these fundamental differences in the microstructural and nanostructural makeups of collagen networks result in qualitatively different mechanical responses under local contact pressure or bulk compression.

Here we investigate how collagen hydrogels deform under both local and bulk compressive loads, comparing their responses to those recently found with pAAm hydrogels.[36] Similar to pAAm hydrogels under locally applied pressure, we find that collagen networks exhibit force−indentation curves that are well described by the Hertz contact model.[37] However, unlike pAAm hydrogels, we find that the elastic moduli determined by these measurements cannot be predicted by classical entropic elasticity models[26] but can be predicted by models of cellular solids.[38] Bulk compression tests also reveal a major difference between collagen and pAAm hydrogels; at applied pressures below the polymer osmotic pressure, pAAm gels are nearly incompressible, while collagen gels exhibit no compressibility threshold that would be associated with an osmotic pressure. We find the ratio between collagen elastic modulus and bulk modulus to be approximately three, corresponding to a Poisson's ratio near zero, indicating that the network compresses along the direction of applied load without significant lateral expansion. Imaging of the collagen networks under applied loads confirms the picture of collagen compression.

MATERIALS AND METHODS

Collagen Network Preparation. A 6.1 mg/mL solution of bovine collagen type I (Nutragen, Advanced BioMatrix) at pH 2−3 is diluted and neutralized with the addition of 10× PBS, 1 N NaOH, and ultrapure deionized water, creating a sample solution having 4.8 mg/mL collagen, 1× PBS, and neutral pH. All solutions are mixed at approximately 2 °C. To create collagen gels, the collagen solution is transferred into either glass-bottom Petri dishes or molds and placed within a cell incubator (5% CO_2, 95% humidity) set at 37 °C for 45 min. Additional cross-linking of gelled collagen is achieved by incubating the cast samples in glutaraldehyde solutions for an additional 45 min within the cell incubator at a 0.5% (w/w) collagen to glutaraldehyde global weight ratio.[39]

Polyacrylamide Gel Preparation. Polyacrylamide hydrogel slabs (d = 20 mm, h = 1 mm) are prepared through free-radical polymerization. A solution containing 7.5% (w/w) acrylamide (AAm; Sigma-Aldrich) as the monomer unit, 0.3% (w/w) *N*,*N*′-methylenebis(acrylamide) (BIS; Sigma-Aldrich) as the cross-linker, 0.15% (w/w) tetramethylethylenediamine (TEMED; Sigma-Aldrich) as the catalyst, and 0.15% (w/w) ammonium persulfate (APS; Sigma-Aldrich) as the free-radical initiator is prepared in ultrapure deionized water. The hydrogel slabs are cast in glass bottom Petri dishes (Cellvis D35-20-0-N) with a cover glass slide placed on top of the solution to minimize the diffusion of oxygen into the solution during the polymerization process. Polyacrylamide hydrogel samples are swollen in ultrapure deionized water to equilibrium over 24 h prior to experimental characterization.

Indentation Measurements. To perform force−indentation measurements with the application of local surface pressures, we use a BioSoft (Bruker) indenter equipped with a 2.5 mm radius sapphire hemisphere. To minimize the forces associated with surface wetting, the samples and the indenting tip are fully submerged in 1× PBS solution. Collagen gels approximately 1 mm thick are prepared as described above and cast by filling the 20 mm diameter imaging wells in 35 mm glass bottomed culture dishes. To reduce adhesion between the indenting probe and the sample, the sapphire hemisphere is cleaned in oxygen plasma and immersed in a 0.1% (w/w) F-127 pluronic solution for several seconds. Samples are indented at a rate of 0.1 μm/s, collecting data on five samples and ten locations per sample. The data capture rate is 100 points/s for both force and displacement. For glutaraldehyde cross-linked samples, the indentation force−displacement (F−d) curves are analyzed using a custom-developed code written in MATLAB,[40] which has better performance in modeling recognizing and fitting compared to the common least-squares fitting methods with an unknown initial point of contact. For non-cross-linked samples, the forces are found be too low to use this method. Instead, we use an autocorrelation analysis method developed for fitting indentation curves, in which the noise in the measured force is comparable to the indentation force.

Bulk Compression Measurements. Bulk compression tests of cross-linked collagen networks are performed by molding sample solutions between roughened, stainless steel, parallel plates on a Malvern Kinexus pro+ rheometer, creating disks 20 mm in diameter and 1 mm in thickness. The combination of roughened stainless-steel plates and thin samples is used to suppress the potential lateral expansion of the collagen samples, ensuring that changes in sample thickness are proportional to changes in sample volume. A stepped loading function is applied, which consists of a loading period of constant displacement rate (0.01 mm/s) followed by a minimum of 10 min relaxation period at a constant level of compression, achieving strains between 0.05 and 0.7. To test whether our results are sensitive to the relaxation period duration, we repeat the loading procedure several times with a longer relaxation period of 1 h, finding no systematic difference in sample response (Figure SI2). The data capturing rate is 100 points/s for both force and displacement. The normal-force transducer of the rheometer is not sensitive enough to measure the response of non-cross-linked collagen gels, so only cross-linked gels are analyzed using this method.

***In Situ* Confocal Reflectance Imaging.** To image potential changes in polymer concentration under locally applied loads, indentation experiments are performed atop an inverted confocal microscope.[36,41,42] We mount a microindentation system with a 2500 μm radius of curvature sapphire indenter probe on an inverted Nikon Ti microscope with a 60× oil objective, achieving a lateral magnification factor of 0.11 μm per pixel with a viewing area of 53 μm × 53 μm. The indenter probe is aligned with the optical axis of the microscope using confocal reflectance optics. To minimize reflections from the sapphire surface, a black-painted or dark-colored indenter probe is used. Images of the collagen are captured over the entire thickness of the sample (typically ∼100 μm) starting with an image focused at the surface closest to glass and afterward increasing the height of the focal plane 0.2 μm in a progressive manner until the top surface is reached (a "z-stack"). Image sets are taken both before indentation and after the sample has been compressed for 1 h to allow for equilibrium to be reached. Comparisons between the fiber relative

https://doi.org/10.1021/acs.langmuir.3c03357
Langmuir 2024, 40, 4228−4235

motion between the strained and unstrained state can then be used to determine strain and divergence.

RESULTS AND DISCUSSION

Indentation Measurements of Collagen Network Elastic Modulus. To characterize the collagen network's response to locally applied pressure, we perform indentation test on 1 mm thick cross-linked and non-cross-linked collagen gel samples prepared at 4.8 mg/mL. Non-cross-linked collagen gels are prepared by casting the collagen solution in a glass bottom Petri dish and incubated in a 37 °C environment for 45 min to induce gelation. Cross-linking of the collagen gel is achieved by incubating the gelled samples in a 0.5% (w/w) glutaraldehyde solution for an additional 45 min; the glutaraldehyde cross-linking of the collagen gel increases the elastic modulus of the collagen fibers without changing the network architecture. We generate curves of applied force, F, versus indentation depth, d, for both the non-cross-linked and cross-linked samples by slowly pressing a hemispherical indentation tip into the collagen gels and measuring the resulting normal force. The collagen gels are submerged in a 1× PBS solution throughout the indentation experiments, and no obvious signs of hysteresis are observed in the loading and unloading force−displacement curves of all samples (Figure SI1).

From the indentation curves, we observe a dramatic contrast in stiffness between the cross-linked and non-cross-linked collagen hydrogels. The cross-linked collagen requires 2 orders of magnitude more force than the non-cross-linked collagen for the same 10 μm deformation (Figure 2a,b). To determine whether a simple contact-mechanics model describes the $F-d$ curve from the cross-linked collagen, we employ a recently developed method that facilitates determining the power-law relationship between force and indentation depth and the elastic modulus of the substrate.[40] Briefly, the F and d data are binned and the numerical derivative of the force with respect to the displacement is taken, defined as F'. This process eliminates the pitfalls of fitting the initial point of contact, and by differentiating the various contact mechanics models, the $F'-F$ power law can be directly mapped to the $F-d$ power law; the $F'-F$ power law exponent is zero for a flat punch, 1/3 for the Hertz model, and 1/2 for the Winkler model. For the cross-linked collagen samples, we find that $F'-F$ scales with a power of 0.326 ± 0.086 (mean ± standard deviation across samples), indicating that the Hertz contact model describes the indentation curves of the cross-linked collagen networks (Figure 2c). We find the elastic modulus of cross-linked collagen samples is E^* = 7.2 ± 1.4 kPa (mean ± standard deviation across samples).

The signal-to-noise ratios in the measured $F-d$ curves from non-cross-linked collagen networks are too low to employ this analysis method because the samples are extremely soft; the noise amplitude is approximately ±20% relative to the mean at the highest measured forces, preventing the binning of the data necessary to compute the numerical derivative. Instead, we employ an autocorrelation analysis method developed for analyzing noisy indentation data.[43] Briefly, we model the measured force as the sum of the contact force described by the Hertz contact model and random noise in the measured force, that is, $F(t) = K\varphi(t) + n(t)$ where $K = \frac{4}{3}E^*R^{1/2}$, $\varphi(t) = d(t)^{3/2}$, and $n(t)$ is the noise in the measured force. By computing the autocorrelation function of each side of this

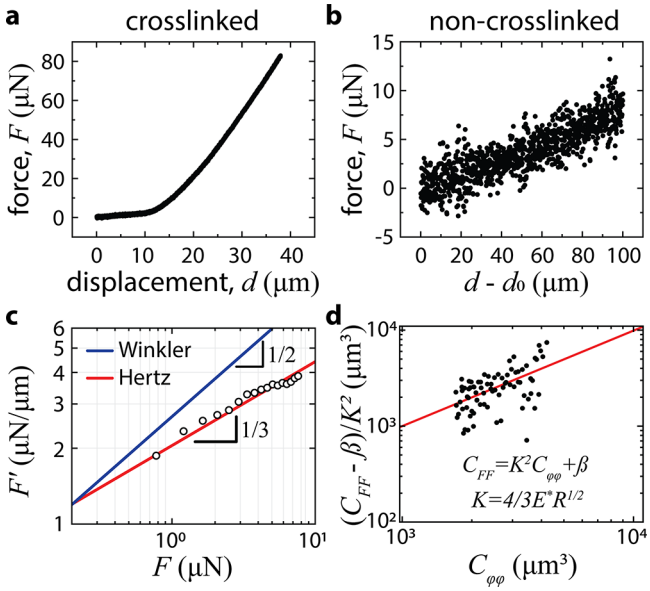

Figure 2. Indentation measurements of the collagen hydrogel networks. (a) and (b) show the representative experimental $F-d$ loading curves for the cross-linked and non-cross-linked collagen samples, respectively. (c) A representative power law fit of the $F'-F$ data for a cross-linked collagen sample. The $F'-F$ data follow a power law relationship with F' scaling like 1/3, consistent with the scaling for the Hertz contact model. We find E^* = 7.2 ± 1.4 kPa for the cross-linked collagen networks (d) Elastic modulus of indentation curves with very low signal-to-noise can be determined by taking the autocorrelation of the indentation force (C_{FF}) and comparing it to the autocorrelation of the displacement ($C_{\varphi\varphi}$). Here, we assume the Hertz contact model and $\varphi(t) = d(t)^{3/2}$. We find E^* = 0.12 ± 0.02 kPa for the non-cross-linked collagen networks. To show all indentation data on a single plot, we fit each data set individually and collapse them as indicated.

equation, we can equate the force autocorrelation function to the sum of the auto- and cross-correlation functions of the indentation depth and the noise, $C_{FF} = K^2C_{\varphi\varphi} + KC_{\varphi n} + KC_{n\varphi} + C_{nn}$. Because the noise in the measured force is random with a mean of 0, we can approximate the autocorrelation and cross-correlation functions involving the noise as a single constant, resulting in a linear relationship between the force autocorrelation function and the displacement autocorrelation function $C_{FF} = K^2C_{\varphi\varphi} + B$, where B is the numerical constant arising from the noise. Here, we apply this analysis technique over the initial few tens of micrometers of the indentation data that corresponds to the linear elastic regime for the Hertz contact model. This linear elastic regime is generally defined as when the indentation depth is much smaller than the contact radius, a. In the Hertz regime of indentation, the contact radius is given by $a = \sqrt{Rd}$, where R is the indenter radius. In our experiments, R = 2.5 mm, so requiring $d/a < 0.1$, we limit our analysis to the first 25 μm of the indentation curve.

We find the elastic modulus of non-cross-linked collagen hydrogels to be E^* = 0.12 ± 0.02 kPa (mean ± standard deviation across samples, Figure 2d), approximately 50 times lower than the cross-linked collagen hydrogels (E^* = 7.2 ± 1.4 kPa). These moduli fall within the range of compressive moduli reported in the literature. The non-cross-linked collagen at 5 mg/mL concentration was reported to have E = 100 Pa.[44] Collagen gels cross-linked at 2.5 mg/mL concentration were reported to have E = 30−12500 Pa over

https://doi.org/10.1021/acs.langmuir.3c03357
Langmuir 2024, 40, 4228−4235

a range of genipin cross-linker concentrations[45] and E = 500−1500 Pa when cross-linked with glutaraldehyde.[39]

Collagen Network Response to Bulk Compression. The fibers constituting collagen networks prepared as described here can be thought of as rigid; the fiber persistence length is many orders of magnitude larger than both the contour length between branches and the mesh size of the networks.[46] The addition of glutaraldehyde cross-linker after the networks have gelled amplifies this disparity in length scales because the network architecture is set before the fibers are stiffened with cross-linker; the primary effect of cross-linker is to further increase the fiber modulus. This rigidity of collagen fibers provides an opportunity to test the potential role of osmotic pressure in a polymer network's resistance to bulk compression. In rigid polymers, thermal fluctuations in chain conformation are suppressed by bending stiffness and contribute negligible resistance to externally applied forces compared with backbone elasticity. By contrast, thermal fluctuations in flexible polymer networks like pAAm are the physical origin of both elasticity and osmotic pressure, which are approximately equal to one another in fully swollen networks.[31]

To experimentally test whether the suppression of polymer thermal fluctuations eliminates osmotic contributions to the bulk compressibility of networks, we measure the amount of pressure required to change their volumes, comparing both pAAm gels to cross-linked collagen networks. While it would be interesting to perform the same measurements on non-cross-linked collagen, the pressures at low levels of volumetric strain are too small to measure with our instrument. Thin samples are cast between roughened parallel plates in a rheometer; the samples are approximately 1 mm thick and 20 mm in diameter. The plates are brought together by incrementally increasing the normal force, reducing sample thickness at each step by 5%−10% at a rate of approximately 1% per second. No lateral expansion of the samples is observed, ensuring that changes in sample thickness generate nearly proportional changes in volume. After each target level of compression is achieved, the sample is allowed to relax for at least 10 min to allow any transient poroelastic effects to dissipate. In collagen gels, we find a linear relationship between normal pressure and compressive strain up to strains of approximately 0.6 (Figure 3). Furthermore, we do not observe strain stiffening behavior of the collagen networks, consistent with previous investigations of collagen networks under compressive loads.[47] These results are averaged from seven samples in which the same sequence of normal loads is applied, and the resulting strains are measured. By contrast, the same experiments on pAAm hydrogels having a comparable elastic modulus of ∼30 kPa exhibit a plateau of nearly incompressible behavior at applied pressures below the network osmotic pressure, Π, as found previously.[36] We determine a bulk modulus, K, of the cross-linked collagen hydrogel from the linear pressure−strain scaling relationship, finding K = 2.2 kPa (Supporting Information). This value is approximately 1/3 the elastic modulus measured from indentation measurements, indicating the network has a very small Poisson's ratio. We estimate Poisson's ratio, ν, by employing the relationship between elastic modulus and bulk modulus from linear elasticity theory, given by. $\nu = (3k - E)/6K$ We estimate the Poisson's ratio of the cross-linked collagen gel to be $\nu = -0.05$. Thus, the suppression of osmotic pressure by increased fiber rigidity appears to enable collagen networks to compress at small applied pressures. In contrast, the response of flexible pAAm polymer networks is dominated by their osmotic pressure at low applied pressures.

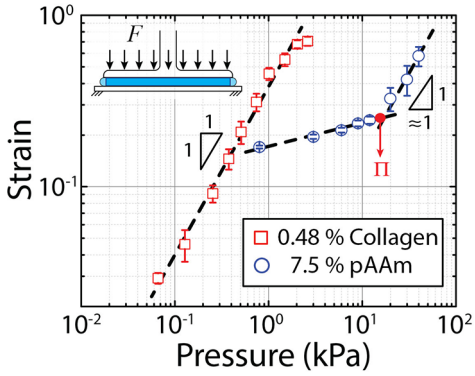

Figure 3. Bulk compression test on both collagen and pAAm hydrogels. Compressive stresses and strains were plotted in log−log space for both 0.48% (w/v) cross-linked collagen and 7.5% (w/w) pAAm samples. It is observed that a transition occurred in pAAm hydrogel samples at a pressure close to their calculated osmotic pressure from mesh size measurement. There is no such transition observed in cross-linked collagen samples. The slopes of the whole collagen curve and the portion above the transition of the pAAm curve are both close to 1, which demonstrates a linear elastic behavior.

***In Situ* Observation of Network Compression under Local Indentation.** To investigate the difference in micro-scale network deformation between collagen and pAAm hydrogels, we perform *in situ* indentation on a confocal microscope to image the deformation of collagen networks under the indenter tip, comparing our results to those from pAAm hydrogels in our previous work.[36] A 4.8 mg/mL concentration collagen hydrogel is cured in a glass-bottom Petri dish and imaged from the bottom (Figure 4a). The sample is compressed over a 2.6 μm displacement by the indenter probe (r = 2500 μm) from the initial point of contact, resulting in a contact diameter of 160 μm. A 53 μm × 53 μm viewing window centered on the apex of the indenter, representing an approximately 140 nm variation in the displacement, is used for the compression analysis, which is less than the vertical resolution of our z-stack (Figure 4b). The captured confocal reflectance images are used to reconstruct the internal fiber structure of the collagen sample (Figure 4b,c). Displacements in the compressed collagen network can be directly seen by overlaying the captured images of the same areas before and after compression and displaying them in false color (Figure 4d,e).

To quantify the deformation and localized strain of the collagen network under indentation, we employ particle image velocimetry methods that capture the relative feature motion in the deformed state. As expected, a smoothly decreasing deformation field along the compression direction is observed (Figure 5a). The local strain in the compression direction is calculated by computing the differences between neighboring displacement vectors along the compression direction and dividing them by their spacing. We find the average strain to be −0.0263 ± 0.0175, with the strain field exhibiting a relatively uniform distribution across the sample and fluctuations over the scale of tens of micrometers (Figure 5b). These fluctuations may correspond to local inhomogeneities within the gel network resulting from gradients in collagen density or reorientation of the collagen fibers.[48,49] However, above this

https://doi.org/10.1021/acs.langmuir.3c03357
Langmuir 2024, 40, 4228−4235

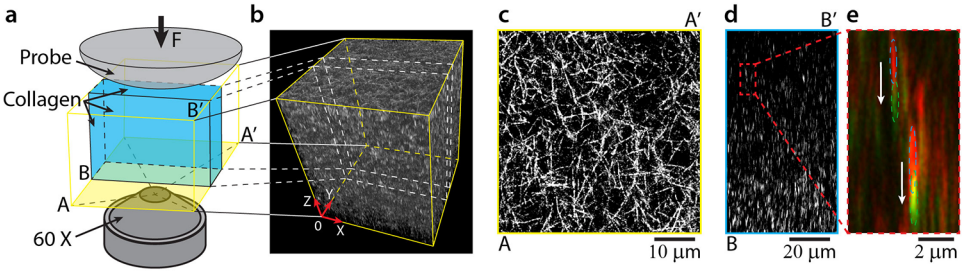

Figure 4. *In situ* confocal observation of the deformation in collagen network under local compression. (a) A representative schematic of the *in situ* confocal indentation setup. (b) A 3D reconstruction of a 53 μm × 53 μm cross-section layered confocal image stack representing the bottom 64 μm of the collagen hydrogel network. (c) Top view image (A−A' plane in (a)) of a single layer of confocal image. (d) Side view image (B−B' plane in (a)) of the collagen network features depicted from a single slice through the reconstructed image stack. The white dots show the cross-sectional areas of collagen fibers. (e) Overlaying of two images with the same observing window captured in the original and compressed states. The image with red features represents the original network, while the image with green features represents the compressed network. The relative motions of some features are marked by dashed circles.

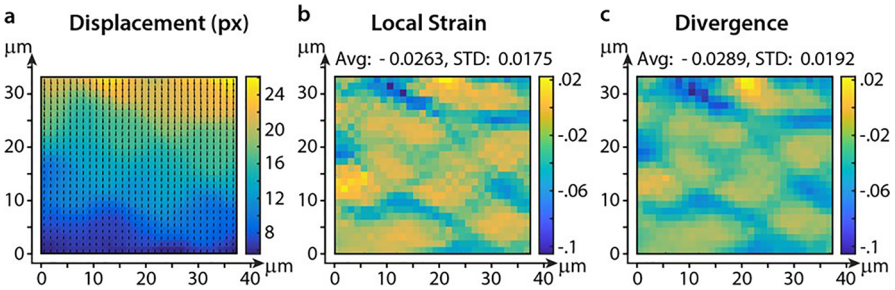

Figure 5. Matlab PIVlab analysis of the indentation displacement, local strain, and divergence of the collagen network. A 37.3 × 33.6 μm^2 subwindow of the course-grain displacement field is shown. (a) Displacement direction (arrows) and magnitude (color gradient) in the confocal window. (b) Local strain along the compression direction is calculated and mapped to 30 × 27 color blocks in the confocal window. Each block contains 24 × 24 pixels, and the magnitude of a block is averaged from all its contained pixels. The axial strain in the confocal window is 0.0263 ± 0.0175 in compression. (c) Local divergence field shows a similar distribution and magnitude as the local axial strain field, indicating the displacement field in the compressed collagen network is dominated by the axial compressive strain with only a small contribution from transverse expansion.

length scale, the strain can be considered globally isotropic, and the collagen network undergoes affine deformation. The spatially resolved divergence in the deformation field exhibits a similar pattern, having an average value of −0.0289 ± 0.0192. The close agreement between the vertical strain field and the divergence indicates the indented collagen network compresses dominantly in the axial direction with very little transverse expansion (Figure 5c). We calculate Poisson's ratio of the collagen network by taking the ratio of the axial contractile strain to the transverse strain and find $\nu \approx 0.0$. This result is consistent with our estimate of the Poisson's ratio from the comparison between the elastic and bulk moduli determined from the local and uniform compression measurements. These results are in stark contrast to the identical experiments previously performed on pAAm gels, where no local volume changes were observed below the contact in response to applied normal loads.

DISCUSSION

Polymers are categorized mechanically from the ratio between the persistence length (l_p) and the contour length (l_c); a polymer chain is considered flexible when $l_p \ll l_c$ and is considered rigid when $l_p \gg l_c$.[50] Most biologically relevant polymers, including f-actin and DNA, fall somewhere between these two extremes and are considered semiflexible with persistence lengths that are comparable to their contour lengths, $l_p \approx l_c$. While individual collagen fibrils have been described as semiflexible,[51] the fibers connecting branches in collagen-1 networks are rigid, having persistence lengths larger than their contour lengths.[46] However, elasticity theory of semiflexible networks is sometimes used to describe collagen networks, so we test it here. The shear modulus of a cross-linked semiflexible polymer network is given by $E' = k_B T l_p^2 l_c^{-3} \xi^{-2}$, where k_B is Boltzmann's constant, T is the temperature, l_p is the persistence length, l_c is the contour length, and ξ is the mesh size of the network. Because collagen networks are branched, we approximate the contour length to be the same as the mesh size, in the range of 1−2 μm as shown in the literature for collagen networks prepared under similar conditions.[27,52,53] Assuming E' = 120 Pa, the modulus of our non-cross-linked samples, this theory would predict that $l_p \approx$ 100−1000 μm. While this persistence length range is consistent with that reported in the literature,[53,54] it is more than 100× the contour length, violating the assumption of semiflexible polymers ($l_p \approx l_c$) and suggesting the collagen networks studied here are considerably more rigid-like. This disparity between the persistence length and contour length is further amplified in the cross-linked collagen hydrogels as the addition of glutaraldehyde after the network has gelled serves to further increase the modulus of the collagen fibers without altering the network's architecture. For the cross-linked collagen hydrogels (E^* = 7 kPa), we find the persistence length predicted from the semiflexible polymer network theory to be $l_p \approx$ 1000−7500 μm, more than 1000× greater than the

https://doi.org/10.1021/acs.langmuir.3c03357
Langmuir 2024, 40, 4228−4235

contour length, again violating the semiflexible assumption. Moreover, the apparent lack of an osmotic pressure further indicates that the role played by thermal fluctuations in semiflexible network mechanics is not significant in collagen networks.

Given the apparent rigidity of the collagen fibers connecting nodes in the network, it may be possible to describe collagen-I gels as cellular solids, where the network elasticity arises from the stiffness of the beam elements with negligible effects from thermal bending. To test whether the theory of cellular solids can be applied to rigid collagen networks, we consider the mechanics model of cellular solids developed by Ashby and Gibson.[38] In this model, the elastic modulus of the cellular structure is determined by the overall effects of element bending rigidity and element relative density compared to its solid state, given by $E_c/E_s = C(\rho_c/\rho_s)^2$, where E_c and E_s are the elastic moduli of the cellular structure and the solid material, respectively, and ρ_c and ρ_s are the corresponding densities. C is an empirical coefficient close to 1. This model assumes an architecture of stiff beam-like elements with a certain nominal length and diameter, connecting to each other the form of a random truss structure, similar to the structural architecture of a collagen network. The Young's modulus of collagen fibers in aqueous conditions has been estimated to be between 3 and 800 MPa for various loading conditions and cross-linking concentrations.[55−58] Applying the known concentrations of the collagen 4.8 mg/mL (relative density of ≈0.5%) with the estimated solid elastic modulus of the cross-linked and non-cross-linked collagen fibers ($E_s \approx 3$ MPa and $E_s \approx 800$ MPa, respectively) leads to an estimated cellular structure modulus of 75 Pa for the non-cross-linked and 20 kPa for the cross-linked collagen networks, within a factor of 3 of the moduli we measure through indentation. We also note that the cellular solid model predicts that the elasticity of collagen networks should scale like the square of collagen concentration; experiments have shown that the power is 2.2, close to this estimate.[47,50,59,60]

Beyond predicting collagen network elasticity, the cellular solid model provides additional insight into the response of such gels to compressive loads. In both the bulk compression measurements and the *in situ* image analysis of collagen indentation, we find the Poisson's ratio of the cross-linked collagen networks to be $\nu \approx 0$. For open-celled structures, such as polymers, open-celled foams, and corks, a Poisson's ratio near zero is often found, where structures compress along the direction of applied load with minimal lateral expansion.[38,61−63] Thus, the mechanics of cellular solids may explain why, unlike flexible polymer networks that are often nearly incompressible, we find that collagen hydrogels behave like rigid networks that volumetrically compress and expel water rather than spreading laterally under large normal loads.

CONCLUSION

In summary, we studied the mechanical response of collagen-I hydrogel networks under localized and bulk compressive loads and compared it to the response of pAAm hydrogels. Similar to pAAm hydrogels, the force−displacement indentation curves of both the cross-linked and non-cross-linked collagen networks can be described by the Hertz contact model for localized compressive loads. However, despite having similar elastic moduli, we find the origins of the elasticity for the pAAm and cross-linked collagen networks to be fundamentally different. The elasticity of pAAM originates from entropic thermal fluctuations of flexible polymer chains between cross-links, while the elasticity of cross-linked collagen networks arises from the bending rigidity of its fibers with minimal contributions from thermal fluctuations. This difference in entropic behavior leads to fundamental differences in their responses to bulk compressive loads and may alter the behavior of cells embedded within these materials. For example, pAAm hydrogels are nearly incompressible at applied pressures below the polymer osmotic pressure, while collagen hydrogels will compress along the direction of the applied load without expanding laterally. Therefore, cells cultured within polyacrylamide hydrogels will experience transverse stresses when a compressive load is applied due to the incompressible nature of the hydrogels made from flexible polymers, while cells within collagen matrices will only experience stresses in the direction of the applied load.

Understanding how these fundamental mechanical differences between pAAm and collagen hydrogels affect cellular behavior will help to guide the development of hydrogel substrates for tribological and biomedical applications. A general conundrum in our understanding of biological interfaces has been articulated by Nicolas Spencer: biotribological surfaces are relatively weak by industrial standards and use poor lubricants (i.e., water), yet are able to withstand large sliding loads with minimal friction.[64] Interestingly, many biointerfaces are composed of an "osmotically active" component like a polymer brush,[65] residing on a microporous substrate like an extracellular matrix network or a layer of living cells.[46,66−68] Our results provide additional understanding of the mechanistic roles played by these different components in biointerfaces *in vivo* and point toward the potential benefits of combining gel phases made from flexible polymers with gel phases made from rigid polymers to create improved biomimicking interfaces for application.

ASSOCIATED CONTENT

Supporting Information

The Supporting Information is available free of charge at https://pubs.acs.org/doi/10.1021/acs.langmuir.3c03357.

Representative force−displacement curve including loading and unloading of cross-linked collagen; representative bulk compression stress−strain response measurement with time-dependent relaxation; bulk vs uniaxial compression modulus analysis (PDF)

AUTHOR INFORMATION

Corresponding Author

Kyle D. Schulze − *Department of Mechanical Engineering, Auburn University, Auburn, Alabama 36849, United States;* orcid.org/0000-0001-8433-0581; Email: kds0069@auburn.edu

Authors

Christopher S. O'Bryan − *Department of Mechanical and Aerospace Engineering, University of Missouri, Columbia, Missouri 65211, United States;* orcid.org/0000-0003-0852-6085

Yongliang Ni − *Department of Mechanical and Aerospace Engineering, University of Florida, Gainesville, Florida 32611, United States*

https://doi.org/10.1021/acs.langmuir.3c03357
Langmuir 2024, 40, 4228−4235

Curtis R. Taylor − *Department of Mechanical and Aerospace Engineering, University of Florida, Gainesville, Florida 32611, United States*

Thomas E. Angelini − *Department of Mechanical and Aerospace Engineering and J. Crayton Pruitt Family Department of Biomedical Engineering, University of Florida, Gainesville, Florida 32611, United States; Department of Materials Science and Engineering, University of Florida, Gainesville, Florida 32603, United States;* orcid.org/0000-0002-0313-4341

Complete contact information is available at: https://pubs.acs.org/10.1021/acs.langmuir.3c03357

Notes

The authors declare no competing financial interest.

■ ACKNOWLEDGMENTS

The authors thank Nicholas Spencer for all of his amazing contributions to our understanding of biotribological and soft interfaces. He has been an invaluable collaborator and friend and a critical sounding board for many dilemmas we have faced in our research.

■ REFERENCES

(1) Drury, J. L.; Mooney, D. J. Hydrogels for tissue engineering: scaffold design variables and applications. *Biomaterials* **2003**, *24*, 4337−4351.
(2) Cohn, D.; Sosnik, A.; Garty, S. Smart hydrogels for in situ generated implants. *Biomacromolecules* **2005**, *6*, 1168−1175.
(3) Kopeček, J. Hydrogel biomaterials: a smart future? *Biomaterials* **2007**, *28*, 5185−5192.
(4) Nicodemus, G. D.; Bryant, S. J. Cell encapsulation in biodegradable hydrogels for tissue engineering applications. *Tissue Engineering Part B: Reviews* **2008**, *14*, 149−165.
(5) Seliktar, D. Designing cell-compatible hydrogels for biomedical applications. *Science* **2012**, *336*, 1124−1128.
(6) Hoffman, A. S. Hydrogels for biomedical applications. *Advanced drug delivery reviews* **2012**, *64*, 18−23.
(7) Caló, E.; Khutoryanskiy, V. V. Biomedical applications of hydrogels: A review of patents and commercial products. *European polymer journal* **2015**, *65*, 252−267.
(8) Pedde, R. D.; et al. Emerging biofabrication strategies for engineering complex tissue constructs. *Adv. Mater.* **2017**, *29*, No. 1606061.
(9) Kandow, C. E.; Georges, P. C.; Janmey, P. A.; Beningo, K. A. Polyacrylamide hydrogels for cell mechanics: steps toward optimization and alternative uses. *Methods in cell biology* **2007**, *83*, 29−46.
(10) Shih, Y. R. V.; Tseng, K. F.; Lai, H. Y.; Lin, C. H.; Lee, O. K. Matrix stiffness regulation of integrin-mediated mechanotransduction during osteogenic differentiation of human mesenchymal stem cells. *Journal of bone and mineral research* **2011**, *26*, 730−738.
(11) Pathak, A.; Kumar, S. Independent regulation of tumor cell migration by matrix stiffness and confinement. *Proc. Natl. Acad. Sci. U. S. A.* **2012**, *109*, 10334−10339.
(12) Fitzgerald, M. M.; Bootsma, K.; Berberich, J. A.; Sparks, J. L. Tunable stress relaxation behavior of an alginate-polyacrylamide hydrogel: comparison with muscle tissue. *Biomacromolecules* **2015**, *16*, 1497−1505.
(13) Dunn, A. C.; Sawyer, W. G.; Angelini, T. E. Gemini interfaces in aqueous lubrication with hydrogels. *Tribol. Lett.* **2014**, *54*, 59−66.
(14) Lee, C. H.; Singla, A.; Lee, Y. Biomedical applications of collagen. *International journal of pharmaceutics* **2001**, *221*, 1−22.
(15) Cancedda, R.; Dozin, B.; Giannoni, P.; Quarto, R. Tissue engineering and cell therapy of cartilage and bone. *Matrix biology* **2003**, *22*, 81−91.
(16) Song, E.; Kim, S. Y.; Chun, T.; Byun, H.-J.; Lee, Y. M. Collagen scaffolds derived from a marine source and their biocompatibility. *Biomaterials* **2006**, *27*, 2951−2961.
(17) Malafaya, P. B.; Silva, G. A.; Reis, R. L. Natural−origin polymers as carriers and scaffolds for biomolecules and cell delivery in tissue engineering applications. *Advanced drug delivery reviews* **2007**, *59*, 207−233.
(18) Ferreira, A. M.; Gentile, P.; Chiono, V.; Ciardelli, G. Collagen for bone tissue regeneration. *Acta biomaterialia* **2012**, *8*, 3191−3200.
(19) Babu, R. P.; O'connor, K.; Seeram, R. Current progress on bio-based polymers and their future trends. *Progress in Biomaterials* **2013**, *2*, 8−16.
(20) Engler, A. J.; Sen, S.; Sweeney, H. L.; Discher, D. E. Matrix elasticity directs stem cell lineage specification. *Cell* **2006**, *126*, 677−689.
(21) Tokita, M.; Tanaka, T. Friction coefficient of polymer networks of gels. *J. Chem. Phys.* **1991**, *95*, 4613−4619.
(22) Reinhart-King, C. A.; Dembo, M.; Hammer, D. A. Endothelial cell traction forces on RGD-derivatized polyacrylamide substrata. *Langmuir* **2003**, *19*, 1573−1579.
(23) Kalcioglu, Z. I.; Mahmoodian, R.; Hu, Y.; Suo, Z.; Van Vliet, K. J. From macro-to microscale poroelastic characterization of polymeric hydrogels via indentation. *Soft Matter* **2012**, *8*, 3393−3398.
(24) Stella, J. A.; D'Amore, A.; Wagner, W. R.; Sacks, M. S. On the biomechanical function of scaffolds for engineering load-bearing soft tissues. *Acta biomaterialia* **2010**, *6*, 2365−2381.
(25) MacKintosh, F.; Käs, J.; Janmey, P. Elasticity of semiflexible biopolymer networks. *Physical review letters* **1995**, *75*, 4425.
(26) Rubinstein, M. Polymer Physics. *Polym. Int.* **2004**, *53*, 1394−1395.
(27) Piechocka, I. K.; van Oosten, A. S.; Breuls, R. G.; Koenderink, G. H. Rheology of heterotypic collagen networks. *Biomacromolecules* **2011**, *12*, 2797−2805.
(28) Piechocka, I. K.; Bacabac, R. G.; Potters, M.; MacKintosh, F. C.; Koenderink, G. H. Structural hierarchy governs fibrin gel mechanics. *Biophys. J.* **2010**, *98*, 2281−2289.
(29) Broedersz, C. P.; MacKintosh, F. C. Modeling semiflexible polymer networks. *Rev. Mod. Phys.* **2014**, *86*, 995.
(30) Jansen, K. A.; et al. The role of network architecture in collagen mechanics. *Biophys. J.* **2018**, *114*, 2665−2678.
(31) Silva, R.; Fabry, B.; Boccaccini, A. R. Fibrous protein-based hydrogels for cell encapsulation. *Biomaterials* **2014**, *35*, 6727−6738.
(32) Reddy, N.; Reddy, R.; Jiang, Q. Crosslinking biopolymers for biomedical applications. *Trends Biotechnol.* **2015**, *33*, 362−369.
(33) Bruck, S. D. Aspects of three types of hydrogels for biomedical applications. *J. Biomed. Mater. Res.* **1973**, *7*, 387−404.
(34) Gibas, I.; Janik, H. Synthetic polymer hydrogels for biomedical applications. *Chem. Chem. Technol.* **2010**, *4*, 297−298.
(35) Peppas, N. A.; Hilt, J. Z.; Khademhosseini, A.; Langer, R. Hydrogels in biology and medicine: from molecular principles to bionanotechnology. *Advanced materials* **2006**, *18*, 1345−1360.
(36) Schulze, K. D.; et al. Polymer osmotic pressure in hydrogel contact mechanics. *Biotribology* **2017**, *11*, 3−7.
(37) Johnson, K. L.; Johnson, K. L. *Contact Mechanics*; Cambridge University Press: 1987.
(38) Ashby, M. F.; Medalist, R. The mechanical properties of cellular solids. *Metallurgical Transactions A* **1983**, *14*, 1755−1769.
(39) Haugh, M. G.; Murphy, C. M.; McKiernan, R. C.; Altenbuchner, C.; O'Brien, F. J. Crosslinking and mechanical properties significantly influence cell attachment, proliferation, and migration within collagen glycosaminoglycan scaffolds. *Tissue Engineering Part A* **2011**, *17*, 1201−1208.
(40) Garcia, M.; et al. Eliminating the surface location from soft matter contact mechanics measurements. *Tribology-Materials, surfaces & interfaces* **2017**, *11*, 187−192.
(41) Schulze, K.; et al. Elastic modulus and hydraulic permeability of MDCK monolayers. *J. Biomech.* **2017**, *53*, 210−213.
(42) McGhee, E. O.; et al. In situ measurements of contact dynamics in speed-dependent hydrogel friction. *Biotribology* **2018**, *13*, 23−29.

(43) O'Bryan, C. S.; Schulze, K. D.; Angelini, T. E. Low force, high noise: Isolating indentation forces through autocorrelation analysis. *Biotribology* **2019**, *20*, No. 100110.
(44) Cross, V. L.; et al. Dense type I collagen matrices that support cellular remodeling and microfabrication for studies of tumor angiogenesis and vasculogenesis in vitro. *Biomaterials* **2010**, *31*, 8596−8607.
(45) Ishihara, S.; Kurosawa, H.; Haga, H. Stiffness-Modulation of Collagen Gels by Genipin-Crosslinking for Cell Culture. *Gels* **2023**, *9*, 148.
(46) Antoine, E. E.; Vlachos, P. P.; Rylander, M. N. Review of collagen I hydrogels for bioengineered tissue microenvironments: characterization of mechanics, structure, and transport. *Tissue Engineering Part B: Reviews* **2014**, *20*, 683−696.
(47) Van Oosten, A. S.; et al. Uncoupling shear and uniaxial elastic moduli of semiflexible biopolymer networks: compression-softening and stretch-stiffening. *Sci. Rep.* **2016**, *6*, No. 19270.
(48) Wen, Q.; Basu, A.; Janmey, P. A.; Yodh, A. G. Non-affine deformations in polymer hydrogels. *Soft Matter* **2012**, *8*, 8039−8049.
(49) Hepworth, D.; Steven-Fountain, A.; Bruce, D.; Vincent, J. Affine versus non-affine deformation in soft biological tissues, measured by the reorientation and stretching of collagen fibres through the thickness of compressed porcine skin. *J. Biomech.* **2001**, *34*, 341−346.
(50) Storm, C.; Pastore, J. J.; MacKintosh, F. C.; Lubensky, T. C.; Janmey, P. A. Nonlinear elasticity in biological gels. *Nature* **2005**, *435*, 191−194.
(51) Rezaei, N.; Lyons, A.; Forde, N. R. Environmentally controlled curvature of single collagen proteins. *Biophys. J.* **2018**, *115*, 1457−1469.
(52) Arevalo, R. C.; Urbach, J. S.; Blair, D. L. Size-dependent rheology of type-I collagen networks. *Biophys. J.* **2010**, *99*, L65−L67.
(53) Yang, Y.-l.; Leone, L. M.; Kaufman, L. J. Elastic moduli of collagen gels can be predicted from two-dimensional confocal microscopy. *Biophys. J.* **2009**, *97*, 2051−2060.
(54) Stein, A. M.; Vader, D. A.; Weitz, D. A.; Sander, L. M. The micromechanics of three-dimensional collagen-I gels. *Complexity* **2011**, *16*, 22−28.
(55) Van Der Rijt, J. A.; Van Der Werf, K. O.; Bennink, M. L.; Dijkstra, P. J.; Feijen, J. Micromechanical testing of individual collagen fibrils. *Macromol. Biosci.* **2006**, *6*, 697−702.
(56) Grant, C. A.; Brockwell, D. J.; Radford, S. E.; Thomson, N. H. Effects of hydration on the mechanical response of individual collagen fibrils. *Appl. Phys. Lett.* **2008**, *92*, 233902.
(57) Andriotis, O. G.; Desissaire, S.; Thurner, P. J. Collagen fibrils: Nature's highly tunable nonlinear springs. *ACS Nano* **2018**, *12*, 3671−3680.
(58) Grant, C. A.; Brockwell, D. J.; Radford, S. E.; Thomson, N. H. Tuning the elastic modulus of hydrated collagen fibrils. *Biophys. J.* **2009**, *97*, 2985−2992.
(59) Morley, C. D.; et al. Quantitative characterization of 3D bioprinted structural elements under cell generated forces. *Nat. Commun.* **2019**, *10*, 3029.
(60) Steinwachs, J.; et al. Three-dimensional force microscopy of cells in biopolymer networks. *Nat. Methods* **2016**, *13*, 171−176.
(61) Shaw, M.; Sata, T. The plastic behavior of cellular materials. *International Journal of Mechanical Sciences* **1966**, *8*, 469−478.
(62) Rinde, J. Poisson's ratio for rigid plastic foams. *J. Appl. Polym. Sci.* **1970**, *14*, 1913−1926.
(63) Markaki, A.; Clyne, T. The effect of cell wall microstructure on the deformation and fracture of aluminium-based foams. *Acta Mater.* **2001**, *49*, 1677−1686.
(64) Lee, S.; Spencer, N. D. Sweet, hairy, soft, and slippery. *Science* **2008**, *319*, 575−576.
(65) Giasson, S.; Spencer, N. D. Aqueous lubrication with polymer brushes. *Aqueous Lubrication* **2014**, 183−218.
(66) Zhang, K.; Simic, R.; Spencer, N. D. Imparting ultralow lubricity to double-network hydrogels by surface-initiated controlled radical polymerization under ambient conditions. *Biotribology* **2021**, *26*, No. 100161.
(67) Simič, R.; Spencer, N. D. Controlling the friction of gels by regulating interfacial oxygen during polymerization. *Tribol. Lett.* **2021**, *69*, 86.
(68) Meier, Y. A.; Zhang, K.; Spencer, N. D.; Simic, R. Linking friction and surface properties of hydrogels molded against materials of different surface energies. *Langmuir* **2019**, *35*, 15805−15812.

NOTE ADDED AFTER ASAP PUBLICATION

This paper published ASAP on February 15, 2024 with an incorrect version of Figure 2. The figure was replaced and the caption updated, and the paper republished when the issue published on February 27, 2024.

https://doi.org/10.1021/acs.langmuir.3c03357
Langmuir 2024, 40, 4228−4235